JTTEE5 19:1163–1170
DOI: 10.1007/s11666-010-9551-7
1059-9630/$19.00 © ASM International

Structure and Tribological Performance of Nanostructured ZrO_2-3 mol% Y_2O_3 Coatings Deposited by Air Plasma Spraying

B. Liang, G. Zhang, H.L. Liao, C. Coddet, and C.X. Ding

(Submitted January 20, 2010; in revised form August 22, 2010)

In this study, nanostructured ZrO_2-3 mol% Y_2O_3 coatings were deposited by air plasma spray using reconstituted feedstock. The coating structures were characterized by x-ray diffractometer, micro-Raman spectrometer, field emission scanning electron microscope, and transmission electron microscope. It is revealed that the as-sprayed coating is mainly composed of columnar grains with diameters <100 nm and demonstrates the better toughness, higher microhardness, and lower porosity. It consists only of nontransformable tetragonal ZrO_2 phase. The tribological performance of the coating was examined with a ball-on-disk apparatus under dry sliding conditions. The results show that the friction coefficient of as-sprayed coating was approximately one-fifth of the conventional zirconia coating and wear rate was lower one order of magnitude than the conventional zirconia coating. The dominant wear mechanism is abrasive wear. The improved wear resistance can be attributed to the increased mechanical properties of as-sprayed coating.

Keywords air plasma spray, nanostructural, tribological properties, ZrO_2 coating

1. Introduction

Zirconia-based ceramic is an excellent biomaterial and has already been used in clinical applications such as the ball heads in total hip replacements. More than 600,000 zirconia-based ceramic femoral heads have been implanted in patients worldwide, mainly in the US and Europe (Ref 1). Recently, zirconia coatings (or films) for biomaterial application has attracted much attention. It is verified that zirconia coatings or films fabricated by air plasma spraying or other methods were in vitro biocompatible (Ref 2-5), and the in vitro biocompatible of the plasma sprayed 3 mol% yttria-stabilized zirconia coating is superior to the bulk ceramic with same composition and has good cytocompatibility (Ref 3, 5). Especially, the nanosized zirconia grains and nanostructured surface can favor the forming of the Zr-OH group, which is believed to be the key to the enhanced bioactivity of plasma sprayed zirconia coating (Ref 3). This implies that the nanostructured zirconia coating has a potential application in clinical field in future. However, if the nanostructured zirconia coatings are used as the clinical coatings, the wear characteristics of coatings should be studied under different conditions. The nanostructured zirconia coating must have an acceptable wear rate and coefficient of friction.

Some research reveals that with the decrease in grain size of zirconia-based ceramic materials, the sliding wear resistance of zirconia-based ceramic material is improved and the relationship between wear resistance of tetragonal zirconia-based ceramic and the grain size is obedient to the type of Hall-Petch law (Ref 6-8). Pioneering investigations have showed that nanostructured ceramic coatings can be achieved using thermal spray techniques as hypersonic plasma deposition (HPPD) (Ref 9), thermal plasma chemical vapor deposition (TPCVD) (Ref 10), suspension plasma spraying (SPS) (Ref 11, 12), high velocity oxy-fuel (HVOF) (Ref 13), electron beam physical vapor deposition (EBPVD) (Ref 14), or air plasma spraying (APS) (Ref 15). Among the aforementioned thermal spray techniques, APS is one of the most important processing techniques currently used to deposit ZrO_2 coating for various applications. It was reported that nanostructured zirconia coating can be achieved by employing proper processing parameters. Thus, in this study, APS has been selected for depositing nanostructured zirconia coating.

This article is an invited paper selected from presentations at the 4th Asian Thermal Spray Conference (ATSC 2009) and has been expanded from the original presentation. ATSC 2009 was held at Nanyang Hotel, Xi'an Jiaotong University, Xi'an, China, October 22-24, 2009, and was chaired by Chang-Jiu Li.

B. Liang, State Key Laboratory of Metastable Materials Science and Technology, Yanshan University, Qinhuangdao 066004, Hebei, People's Republic of China; **B. Liang** and **G. Zhang**, Institute for Composite Materials, University of Kaiserslautern, 67663 Kaiserslautern, Germany; **G. Zhang, H.L. Liao,** and **C. Coddet**, LERMPS, Université de Technologie de Belfort-Montbéliard, 90010 Belfort, France; and **C.X. Ding**, Shanghai Institute of Ceramics, Chinese Academic of Sciences, Shanghai 200050, People's Republic of China. Contact e-mail: liangbo@ysu.edu.cn.

The objectives of this study are to characterize the structure of nanostructured 3 mol% yttria-stabilized zirconia coating deposited by APS using reconstituted feedstock and to examine the sliding tribological performance of the as-sprayed coating under dry sliding conditions.

2. Experimental Procedures

2.1 Coating Preparation

Commercial nanoscale powders of 3 mol% yttria-stabilized zirconia with the mean diameter of 50 nm (Farmeiya Advanced Materials Co. Ltd., Jiujiang, China) were used as raw materials. Before thermal spraying, the nanoscale zirconia powders were reconstituted into granules with the mean diameter of 60 μm by a spray drying process. The coatings were deposited with the help of a Metco A-2000 atmospheric plasma spray system (Sulzer Metco AG, Zurich, Switzerland). Medium carbon steel disk and stainless steel rod were used as substrates. The former substrate is used to deposit wear test specimens and the latter is to deposit adhesion test specimens as described below. The medium carbon steel disk has a 65 mm diameter and a 5 mm thickness. The stainless steel rod has a diameter of 25.4 mm. The substrates were grit-blasted with white corundum and degreased ultrasonically in acetone before spraying. During spray process, the disks were fixed in front of the torch which scanned with a linear velocity of 200 mm/s. A uniform design experiment based on number-theoretic methods was used to optimize the spraying parameters according to coating microhardness (Ref 16). The optimized spraying parameters are listed in Table 1.

2.2 Characterizations of the Structures, Physical, and Mechanical Properties of the Coatings

The as-sprayed coatings were inspected with a transmission electron microscopy (TEM, JEM-200CX Jeol, Tokyo, Japan) and the surface was examined with a field emission scanning electron microscope (FESEM, JSM-6700F, Jeol, Tokyo, Japan). The phase composition was detected by a RAX-10 x-ray diffractometer (XRD, Rigaku, Tokyo, Japan) operating with Cu Kα ($\lambda = 0.154056$ Å) and a LabRam-1B micro-Raman spectrometer (Dilor, Lille, France). The radiation of the 632.8 cm^{-1} line from a He-Ne laser was used as the excitation source and with 6.4 mW incident power and 100 s for each specimen. The porosity of the as-sprayed coating was estimated by quantitative image analysis (IA). Ten of polished cross-section micrographs were used to calculate the porosity. The adhesive strength of the as-sprayed coatings was measured using a materials tester (50 KN load cell, Model 11/2612, Zwick, Germany) in accordance with ASTM C 633-79 standard. A thin layer of E-7 adhesive glue (Huayi, Shanghai, China) having a tensile strength higher than 70 MPa was applied. The final value represented the average of five samples. The Vickers microhardness was measured using a HX-1000 microhardness tester (Jinpeng, Shanghai, China) on polished cross-section of the coating with a load 0.2 kg for duration time 15 s. The average microhardness was calculated from 20 repeats. The elastic modulus was determined by the Instron-5566 system (Instron, Grove City, America), and the average elastic modulus was calculated from five measurements. Surface roughness measurements were conducted with 0.5 mm/s traverse speed at 4.8 mm length using a TK300 HOMMEL Roughness Tester (Wave, Hommelwerke GmbH, Germany).

Table 1 The optimal plasma spraying parameters

Ar, Slpm	40
H_2, Slpm	12
Carrier gas flow, Slpm	3.5
Current, A	620
Power, KW	42
Powder feed rate, g/min	19
Spraying distance, mm	120

2.3 Friction and Wear Tests

Sliding tribological tests were performed using a ball-on-disk arrangement (CH-2000 tribometer, CSEM, Neuchatel, Switzerland). The counterpart was a 6 mm diameter 100C6 steel ball. Prior to the test, the coatings were ground using grit SiC papers and then polished using diamond slurries down to a mean surface roughness of 0.1 to 0.4 μm. During the test, the friction force was measured with a sensor and fed into a computer dynamically at a frequency of 12 data per min. The friction coefficients were obtained when the measured forces were divided by the applied load. The tests were conducted at room temperature and lab air environment. The applied loads of 5, 9, and 15 N, sliding speeds of 0.5, 0.8, and 1.1 m/s, respectively, were selected to investigate their influence on the friction and wear behavior. The wear rates represent the worn volumes per unit of the applied load and the sliding distance. The cross-section areas were calculated from the section profile of the wear tracks measured using a Taylor-Hobson Surtronic 3P profilmeter (Rand Taylor Hobson Ltd., Leicester, UK). The multiplication of the cross-section area by the perimeter of the wear track gives the total worn volume. For each parameter, at least three repetitive tests were performed for calculating the mean wear rate. The worn surfaces of coatings and 100C6 steel ball were also analyzed with an EPMA-8705QH scanning electron microscopy (SEM, Shimadzu, Tokyo, Japan) and by an INCA energy-dispersive spectrometer (EDS, Oxford Instruments, High Wycombe, UK).

3. Results and Discussion

3.1 Coating Characteristics

Figure 1 presents the TEM micrographs of as-sprayed coating. From Fig. 1(a), it can be clearly seen that as-sprayed ZrO_2 coating is mainly composed of irregular-shaped fine equiaxed grain with the grain size range from

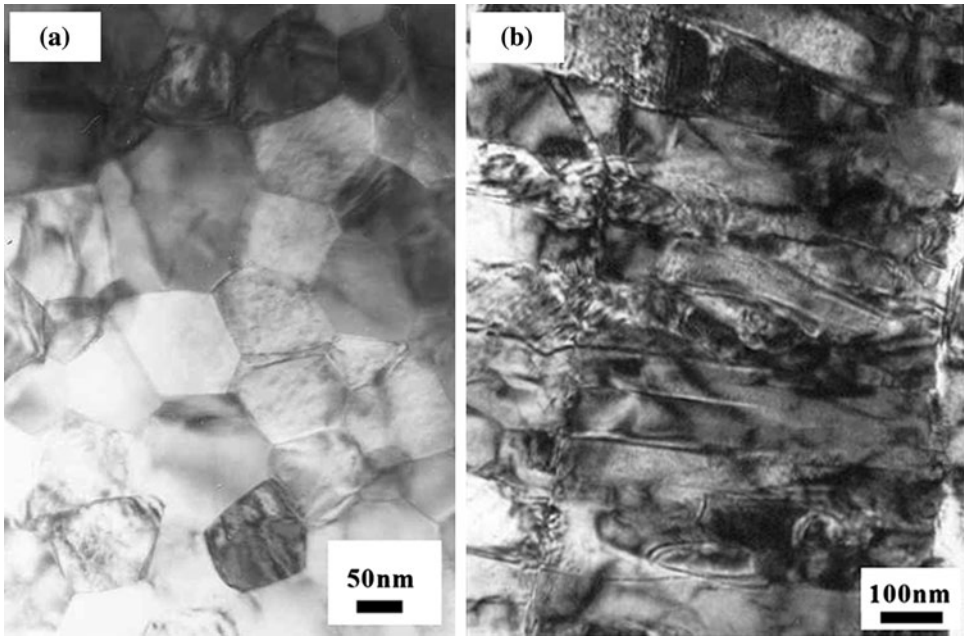

Fig. 1 TEM micrographs of plasma sprayed nanostructured zirconia coating (a) vertical to spraying direction (b) parallel to spraying direction

50 to 150 nm. As shown in Fig. 1(b), the diameter of columnar grains ranges from 50 to 100 nm and their average length is larger than 300 nm. Therefore, it can be concluded that the as-sprayed coating has a nanostructure.

It is generally accepted that the fine grains were formed as a result of homogenous nucleation and propitiation from a highly undercooled melt and columnar grain growth arises from heterogeneous nucleation at splat boundaries where exist a higher gradient of cooling rate and rapid growth into molten splat (Ref 17). The fact why the ZrO_2 coating sprayed with nanosize powders presents smaller grain sizes is still unclear. Surely, this will be an important issue for current and future studies. However, the nanostructure obtained in this study is verified to be useful for improving bioactivity of the coating (Ref 3).

Figure 2(a) presents the SEM micrograph of as-sprayed coating without polishing. It can be seen from Fig. 2(a) that the as-sprayed coating without polishing is smooth. The surface roughness (*Ra* value) is 6.03 ± 0.17 μm. This infers that the reconstituted powders have a good melting state before spreading. It has been verified that the abrasion resistance of thermal sprayed coatings is related to the relative fracture toughness and the indentation fracture method is often employed to characterize the relative fracture toughness of coatings (Ref 18). Figure 2(b) presents the morphology of the Vickers indentation observed in as-sprayed coating. It can be seen from Fig. 2(b) that many microcracks were observed around the indentation, and some microcracks branched as arrow indicated in Fig. 2(b). Based on the mechanism of microcrack-toughening (Ref 19), the more the microcracks and branching cracks, the more energy of crack propagating can be absorbed. This means that the nanostructured zirconia coating posses a higher fracture toughness. Secondly, the nanostructure of as-sprayed zirconia coating can also result in the improvement of fracture toughness due to the increase of cracks propagation distance along the grain boundary. Thirdly, it was verified that there exist many microcracks in plasma sprayed nanostructured 3 mol% yttria-stabilized zirconia coating (Ref 20). These microcracks can act as crack arrestors which may inhibit the crack growth generated due to indentation test.

Figure 2(c) presents the low-magnification SEM image of the coating cross-section. From the morphology of cross-section area, it can be seen that the bonding between coating and substrate is excellent. The adhesion strength detected was 24 ± 3.2 MPa (as listed in Table 2). The coating possesses two kinds of pores. One is some larger pore, which is larger than 10 μm, and the other is small ball-like pores of less than 1 μm and homogeneous distribution. The porosity of the as-sprayed coating is approximately 9.05% with the standard deviation of ±1.85, which was lower than that of conventional zirconia coating (Ref 21).

The physical and mechanical properties of nanostructured ZrO_2 coatings obtained in this study are listed in Table 2. If comparing with those of conventional ZrO_2 coatings (Ref 21), the nanostructured ZrO_2 coating displays the better properties, such as the lower porosity, the higher microhardness.

Figure 3(a) shows the XRD spectra of the as-sprayed coating. It is clearly seen that the nanostructured zirconia coating is composed only with tetragonal zirconia phase, the monoclinic zirconia phase detected in starting powder was disappear after spraying. This result was also verified by Raman spectrum analysis technology. It is reported that the tetragonal and monoclinic polymorphs of zirconia have distinct and characteristic Raman spectra. A small

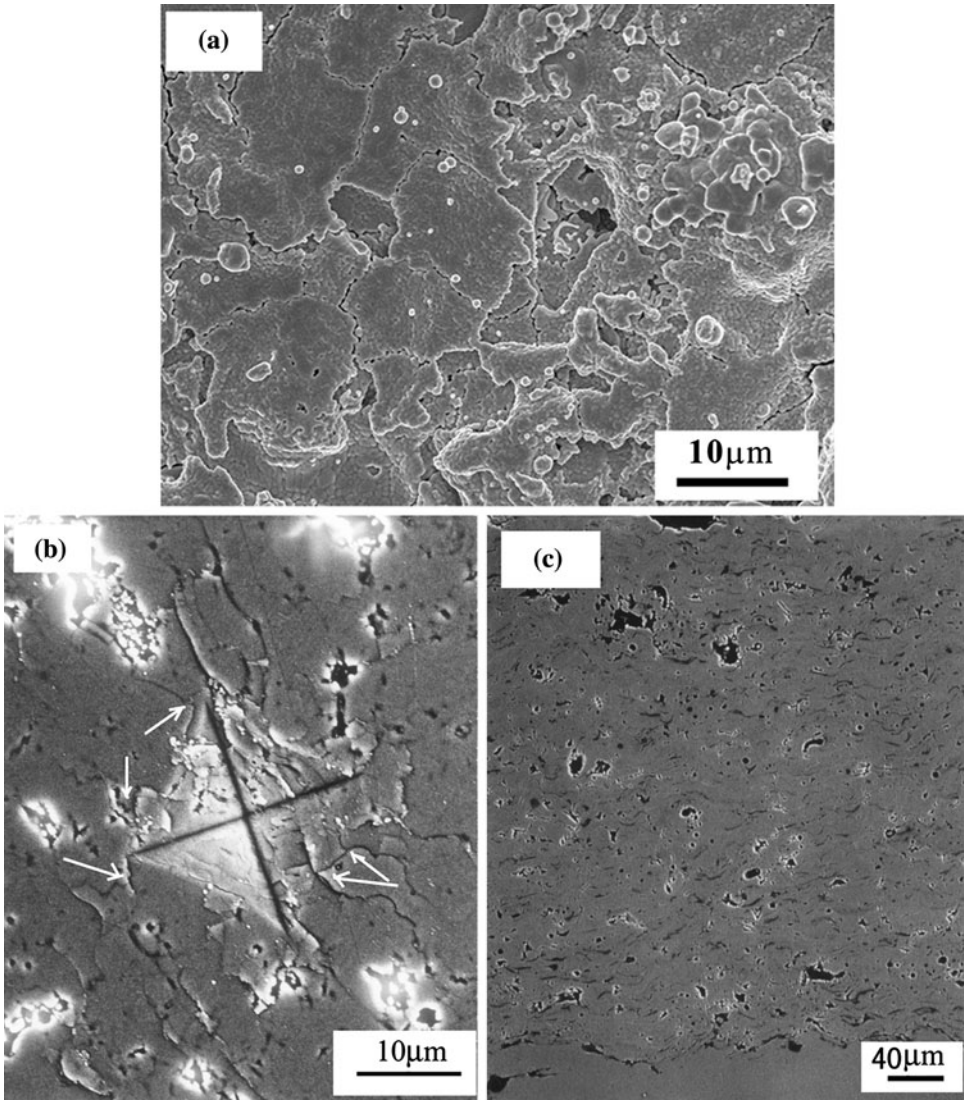

Fig. 2 The morphology of plasma sprayed nanostructured zirconia coating (a) FESEM morphology of surface (b) SEM image of the Vickers indentation, and (c) SEM image of cross-section area

Table 2 Physical and mechanical properties of nanostructured ZrO_2 coating

Nanostructured ZrO_2 coating				
Porosity, %	Roughness, μm	Adhesion strength, MPa	Microhardness, GPa	Young's modulus, GPa
9.05 ± 1.85	6.03 ± 0.17	24 ± 3.2	6.36 ± 0.73	31.8 ± 1.91

amount of tetragonal or monoclinic phase could be detected in a polycrystalline zirconia material by its distinguishing lines. The monoclinic doublet (at 181 and 192 cm^{-1}) and the tetragonal bands (around 148 and 264 cm^{-1}) are well separated over the range 100 to 1000 cm^{-1}. Figure 3(b) presents the Raman spectra of as-sprayed coating. From Fig. 3(b), it can be seen that no characteristic Raman lines of monoclinic and cubic phase were observed. Four Raman lines occurred at 153.7, 261.1, 472.8, and 642.8 cm^{-1} were identified with the typical characteristics of tetragonal phase. In fact, this tetragonal zirconia phase was so-called nontransformable tetragonal phase (Ref 20), which is stable if aging in water at temperature less than 313 k (Ref 22). This result is important for clinical application of coating because the body temperature would be never higher than 315 k.

3.2 Tribological Properties

Figure 4 shows the variation of friction coefficient with the sliding distance at 0.5, 0.8, and 1.1 m/s under applied load of 5, 9, and 15 N, respectively. From Fig. 4, it can be seen that, during the test of sliding velocities, the curves of nanostructured ZrO_2 coatings under applied loads of 5 and 9 N are obviously different from those under 15 N.

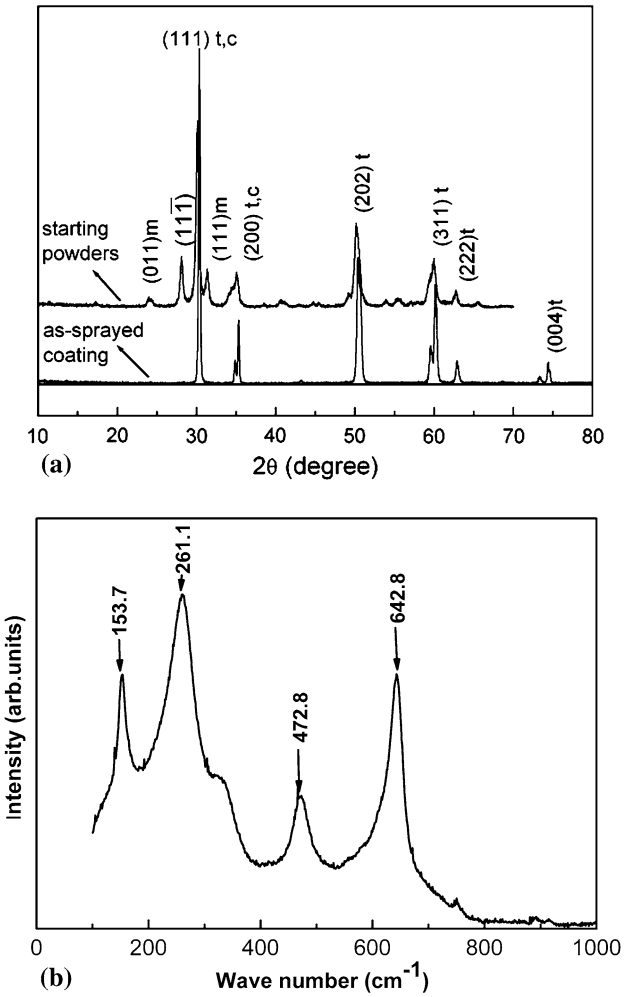

Fig. 3 XRD spectra (a) and Raman spectrum (b) of plasma sprayed nanostructured zirconia coating

When comparing the curves of friction coefficient under 5 N with those obtained at applied of 9 N at 0.5 m/s (Fig. 4a), 0.8 m/s (Fig. 4b) and 1.1 m/s (Fig. 4c), it can be clearly seen that the friction coefficient variation trends are very similar. The friction coefficients obtained under applied 5 and 9 N do not increase or decrease with the increase of sliding distance, indicating that the final stage of wear process—failure stage is not reached after 2000 m sliding distance. However, when the applied load is increased to 15 N, the friction coefficient variation trend is remarkable different from that obtained under 5 and 9 N. As shown in Fig. 4(a), a sudden increase of friction coefficient after 1500 m sliding distance can be seen from the friction coefficient curve obtained under 15 N at 0.5 m/s. After the maximum friction coefficient value is reached, the friction coefficient gradually decreases with the increase of sliding distance. It can be deduced that friction coefficient would reach a steady-state value finally. This transition of friction coefficient is closely related to the transition of wear state. In general, this sudden increase of friction coefficient indicates the wear state transfers from

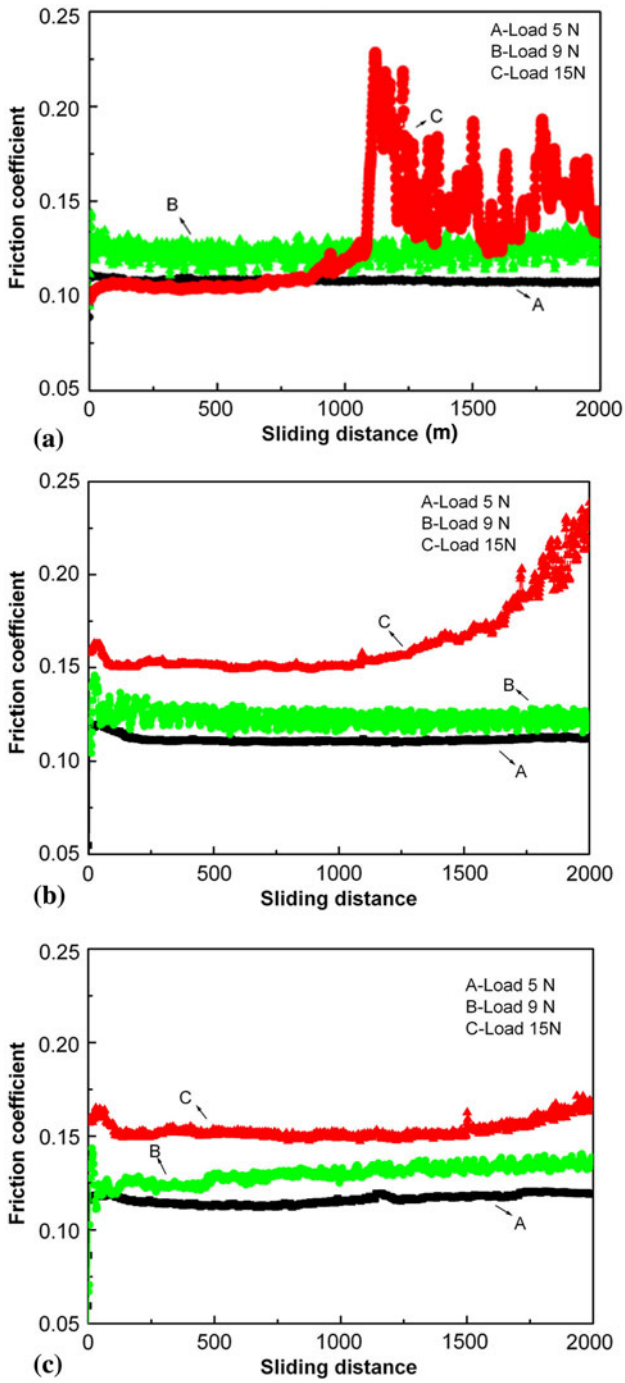

Fig. 4 The coefficient of friction traces of plasma sprayed nanostructured coating under the applied load of 5, 9, and 15 N at sliding velocity of (a) 0.5 m/s, (b) 0.8 m/s, and (c) 1.1 m/s

mild state to severe state due to the change of wear mechanism, which will be discussed in the next section. This transition was also observed in Fig. 4(b). From Fig. 4(b), the friction coefficient value obtained under 15 N was also rapidly increased after about 1500 m sliding distance, and it seems that the peak value has not been reached after 2000 m sliding distance. This is different

with what was observed in Fig. 4(a), however, it also shows the mild to severe state transition.

The most attractive phenomenon is that when the sliding velocity reaches to 1.1 m/s (as shown in Fig. 4c), the transition observed in Fig. 4(a) and (b) under 15 N seems disappeared. In fact, the decrease of friction coefficient can be attributed to the existence of wear debris occurred under high applied load, which may act as a lubricant with an effect of load-carrying in terms of lower friction coefficient. Detail discussion will be given in the following sections.

In addition, Fig. 4 also reveals that the friction coefficient may increase with the increase of applied load. The applied load plays very important role in the wear process of nanostructured ZrO_2 coatings. When the applied load is reached over a critical value, the applied load would result in the transition from mild to severe state.

3.3 Wear Mechanism

The foregoing experimental results show that the plasma sprayed nanostructured ZrO_2 coatings deposited from spray-dried nanosize powders have outstanding tribological properties. In order to determine which wear mechanism occurred during the wear process, the worn surfaces of plasma sprayed nanostructured ZrO_2 coatings, counterpart ball, and wear debris were examined with the SEM.

Figure 5 presents the typical morphology of worn surface of nanostructured ZrO_2 coatings and counterpart ball after sliding under a load of 9 N at 0.8 m/s. From Fig. 5(a), it can be seen that local brittle fracture took place on the worn surface of plasma sprayed nanostructured zirconia coating and the fine-size debris was clearly observed on the worn surface of counterpart ball (Fig. 5b). This indicates that the wear mechanism is a combination of abrasive wear and brittle fracture. In general, brittle fracture during wear testing always resulted from a worse cohesion and lower toughness of coating materials, however, the forgoing experiment shows that plasma sprayed nanostructured zirconia coating demonstrates a higher cohesion strength, lower porosity, and higher microhardness (as listed in Table 2). It is accepted that the wear resistance properties of zirconia ceramic material increase with decrease of its grain size and porosity, the increase of adhesion strength as well as microhardness, especially the decrease of grain size (Ref 23-25). In this study, TEM examination results reveal that the as-sprayed coating possesses much finer grain (as shown in Fig. 1), and porosity was lower. So, the dominant wear mechanism of plasma sprayed nanostructured zirconia coating comes from abrasive wear, not brittle fracture. Under dry conditions, the wear debris plays a crucial role in wear properties of plasma sprayed zirconia coating. The wear debris remaining in wear contact area was considered as ''third body,'' which could form an adherent layer. This adherent layer could protect the underneath coatings and decrease the wear in following tests (Ref 26). In order to examine characteristics of wear debris, some debris were collected and analyzed with FESEM. The morphologies of debris were presented in Fig. 6(a). It can be seen from Fig. 6(a) that most wear debris particles were less than 1 μm and globular. This was in agreement with the observation in Fig. 5(b). The EDS analysis suggests that the debris mainly arises from the nanostructured zirconia coating. However, Fe and Cr elements were also clearly observed, indicating the metal element transfer from counterpart ball to coating surface (Fig. 6b). Under dry sliding conditions in air atmosphere, Fe and Cr elements

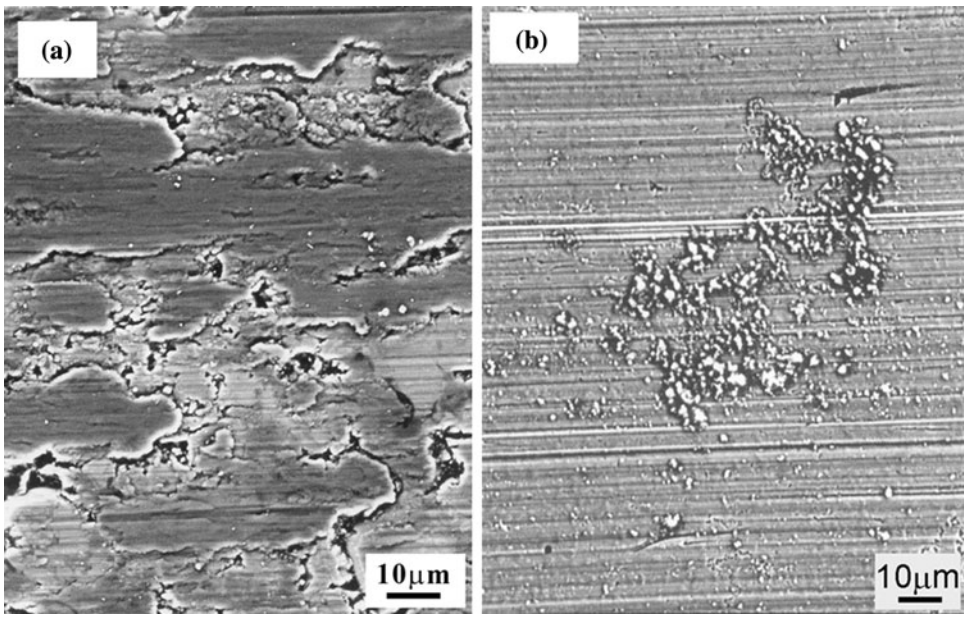

Fig. 5 SEM micrographs of worn surface (a) plasma sprayed nanostructured zirconia coating and (b) counterball surface under load 9 N at 0.8 m/s

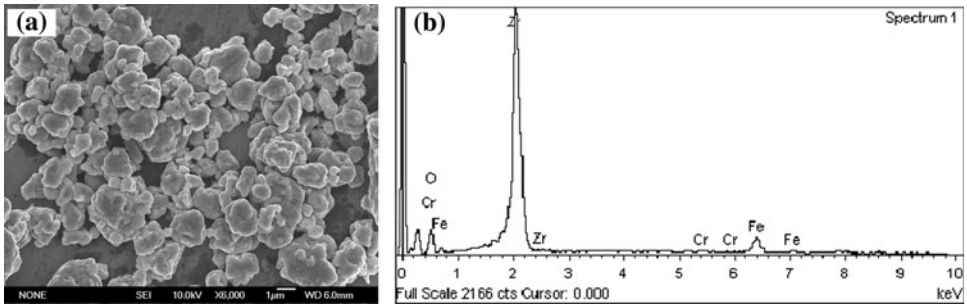

Fig. 6 FESEM micrograph of worn debris (a) and (b) EDS result

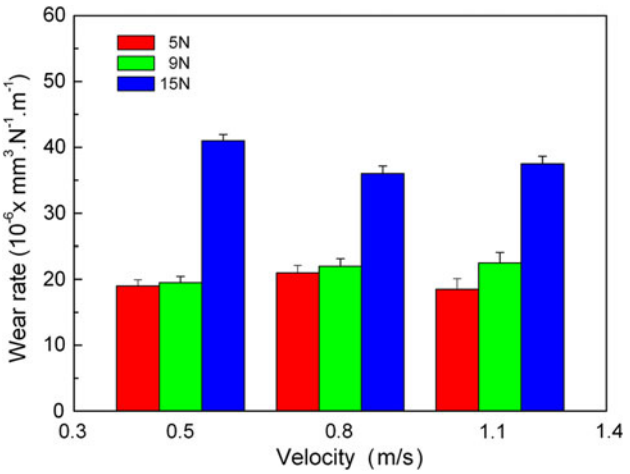

Fig. 7 Wear rate of plasma sprayed nanostructured zirconia coating under the applied load of 5, 9, and 15 N at 0.5, 0.8, and 1.1 m/s

may react with oxygen, forming Fe_2O_3 and Cr_2O_3. So, the debris is composed of zirconia abrasive particles and a small amount of ferric and chrome oxide.

The wear rate versus applied load and sliding velocity was presented in Fig. 7. It can be seen from Fig. 7 that the wear rate of as-sprayed coating is closely related with applied loads. Under the applied load of 15 N, the wear rate value is considerably higher than those obtained at 5 and 9 N. The effect of sliding velocity on wear rate is not serious in this study, if comparing with the effect of applied load. This is an interesting phenomenon. We think this maybe lie in the adherent layer formed in sliding process, which can acts as a lubricant, resulting in the lower wear rate and lower coefficient of friction. However, this phenomenon needs to be studied systematically.

It is important to compare the above results with those obtained in our laboratory (Ref 27). Through the comparison, it can be found that the friction coefficients obtained in this study are about one-fifth of those of the plasma sprayed conventional coating and the wear rates are lower about one order of magnitude than those of conventional coatings. This indicates that the nanostructured coating has superior tribological performances, i.e., lower friction coefficient and wear rate, than conventional zirconia coating.

4. Conclusions

Plasma sprayed nanostructure zirconia coating was deposited using reconstituted feedstock. The as-sprayed coating is composed of only with tetragonal phase. It displays the better properties, such as the better toughness, lower porosity, higher microhardness, and adhesion strength.

The nanostructured zirconia coatings demonstrate the superior wear properties. Its friction coefficient can be reduced to 0.2 under the dry conditions. The dominant wear mechanism is characterized by abrasive wear. The analysis on the worn surface revealed that the wear properties were closely with the properties of as-sprayed coating. The improved wear resistance can be attributed to the increased mechanical properties of as-sprayed coating.

References

1. J. Chevalier, What Future for Zirconia as a Biomaterial?, *Biomaterials*, 2006, **27**, p 535-543
2. R.S. Lima and B.R. Marple, Thermal Spray Coatings Engineered from Nanostructured Ceramic Agglomerated Powders for Structural, Thermal Barrier and Biomedical Applications: A Review, *J. Thermal Spray Technol.*, 2007, **16**(1), p 40-63
3. G.C. Wang, X.Y. Liu, J.H. Gao, and C.X. Ding, In Vitro Bioactivity and Phase Stability of Plasma-Sprayed Nanostructured 3Y-TZP Coatings, *Acta Biomater.*, 2009, **5**, p 2270-2278
4. W.F. Li, X.Y. Liu, A.P. Huang, and P.K. Chu, Structure and Properties of Zirconia (ZrO2) Films Fabricated by Plasma-Assisted Cathodic Arc Deposition, *J. Phys. D Appl. Phys.*, 2007, **40**, p 2293-2299
5. G.H. Wang, X.Y. Liu, and C.X. Ding, Phase Composition and In Vitro Bioactivity of Plasma Sprayed Calcia Stabilized Zirconia Coatings, *Surf. Coat. Technol.*, 2008, **202**, p 5824-5831
6. K.H. Zum Gahr, W. Bundschuh, and B. Zimmerlin, Effect of Grain Size on Friction and Sliding Wear of Oxide Ceramics, *Wear*, 1993, **162-164**, p 269-279
7. G.S.A.M. Theunissen, J.S. Bouma, A.J.A. Winnubst, and A.J. Burggraag, Mechanical Properties of Ultra-Fine Grained Zirconia Ceramics, *J. Mater. Sci.*, 1992, **27**(14), p 4429-4438
8. L.L. Shaw, D. Goberman, R. Ren, M. Gell, S. Jiang, Y. Wang, T. Danny Xiao, and P.R. Strutt, The Dependency of Microstructure and Properties of Nanostructured Coatings on Plasma Spray Conditions, *Surf. Coat. Technol.*, 2000, **130**, p 1-8
9. N.P. Rao, H.J. Lee, D.J. Hansen, J.V.R. Heberlein, P.H. McMurry, and S.L. Girshick, Nanostructured Materials Production by Hypersonic Plasma Particle Deposition, *Nano-structured Mater.*, 1997, **9**, p 129-132

10. Z.P. Lu, J. Heberlein, and E. Pfender, Process Study of Thermal Plasma Chemical Vapor Deposition of Diamond, Part 1: Substrate Materials, Temperature, and Methane Concentration, *Plasma. Chem. Plasma Process.*, 1992, **12**, p 35-53
11. F. Gitzhofer, E. Bouyer, and M. I. Boulos, Suspension Plasma Spray Deposition, US Patent No. 5,609,921 (1997)
12. J.O. Berghaus, B.R. Marple, and C. Moreau, Suspension Plasma Spraying of Nanostructured WC-12Co Coatings, *J. Thermal Spray. Technol.*, 2006, **15**(4), p 676-681
13. R.S. Lima and B.R. Marple, Superior Performance of High-Velocity Oxyful-Sprayed Nanostructured TiO_2 in Comparison to Air Plasmas-Sprayed Conventional Al_2O_3-13TiO_2, *J. Thermal Spray Technol.*, 2005, **14**(3), p 397-404
14. X. Zhao, X. He, Y. Sun, J. Yi, and P. Xiao, Superhard and Tougher SiC/Diamond-Like-Carbon Composite Films Produced by Electron Beam Physical Vapor Deposition, *Acta Mater.*, 2009, **57**, p 893-902
15. H. Chen and C.X. Ding, Nanostructured Zirconia Coating Prepared by Atmospheric Plasma Spraying, *Surf. Coat. Technol.*, 2002, **150**, p 31-36
16. K.T. Fang and Y. Wang, *Number-Theoretic Methods in Statistics*, Chapman and Hall, London, 1993
17. P.D. Harmsworth and R. Stevens, Microstructure of Zirconia-Yttria Plasma-Sprayed Thermal Barrier Coatings, *J. Thermal Spray Technol.*, 1995, **4**(3), p 245-251
18. A. Karimi, Ch. Verdon, and G. Barbezat, Microstructure and Hydroabrasive Wear Behaviour of High Velocity Oxy-Fuel Thermally Sprayed WC-Co(Cr) Coatings, *Surf. Coat. Technol.*, 1993, **57**, p 81-89
19. A. G. Evans, Toughening Mechanisms in Zirconia Alloys, *International Conference on the Science and Technology of Zirconia* (2nd, 1983, Stuttgart, Germany), *Science and Technology of Zircionia II, Advances in Ceramics*, Vol 12, N. Claussen and M. Rühle Ed., The American Ceramic Society, Inc., Columbus, OH, 1984, p 193-212
20. B. Liang and C.X. Ding, Phase Composition of Nanostructured Zirconia Coatings Deposited by Air Plasma Spraying, *Surf. Coat. Technol.*, 2005, **191**, p 267-273
21. H. Chen, Y.F. Zhang, and C.X. Ding, Tribological Properties of Nanostructured Zirconia Coatings Deposited by Plasma Spraying, *Wear*, 2002, **253**, p 885-893
22. B. Liang, C.X. Ding, H.L. Liao, and C. Coddet, Study on Structural Evolution of Nanostructured 3 mol% Yttria Stabilized Zirconia Coatings During Low Temperature Ageing, *J. Euro. Ceram. Soc.*, 2009, **29**, p 2267-2273
23. C.T. Yang and W.J. Wei, Effects of Material Properties and Testing Parameters on Wear Properties of Fine Grain Zirconia, *Wear*, 2000, **242**, p 97-104
24. J.E. Hines, Jr., R.C. Bradt, and J.V. Biggers, Grain Size and Porosity Effects on the Abrasive Wear of Alumina, *Wear of Materials*, W.A. Glaeser, K.C. Ludema, and S.K. Rhee, Ed., American Society of Mechanical Engineers, New York, 1977, p 462-467
25. Y. He, L. Winnubst, A.J. Burggraaf, H. Verweij, P.G.Th. Varst, and B. With, Influence of Porosity on Friction and Wear of Tetragonal Zirconia Polycrystal, *J. Am. Ceram. Soc.*, 1997, **80**(2), p 377-380
26. G.W. Stachowiak, G.B. Stachowiak, and A.W. Batchelor, Metallic Film Transfer During Metal-Ceramic Unlubricated Sliding, *Wear*, 1989, **132**, p 361-381
27. H. Chen, S. Lee, X. Zheng, and C. Ding, Evaluation of Unlubricated Wear Properties of Plasma-Sprayed Nanostructured and Conventional Zirconia Coatings by SRV Tester, *Wear*, 2006, **260**, p 1053-1060